Emission of Muonium into Vacuum from a Silica-Powder Layer

G. A. Beer, G. M. Marshall,[a] G. R. Mason, and A. Olin[a]

University of Victoria, Victoria, British Columbia V6R 2C9, Canada

Z. Gelbart and K. R. Kendall

TRIUMF, Vancouver, British Columbia V6T 2A3, Canada

T. Bowen, P. G. Halverson, and A. E. Pifer

University of Arizona, Tucson, Arizona 85721

C. A. Fry[b] and J. B. Warren

University of British Columbia, Vancouver, British Columbia V6T 1W5, Canada

and

A. R. Kunselman

University of Wyoming, Laramie, Wyoming 82071

(Received 12 May 1986)

Muonium atoms have been observed in vacuum after emission from a layer of finely divided silica powder. By extrapolation of the decay-positron track, both the time and position of muon decay are measured, confirming thermal emission at room temperature. The yields range up to $(19 \pm 6)\%$ of muons stopping in the layer, depending on its thickness. The result is used to recalculate the upper limit for conversion of muonium to antimuonium.

Muonium is a hydrogenlike atom consisting of a positive muon and an electron. The structureless leptonic nature of the muon makes muonium ideal for testing certain aspects of weak and electromagnetic interactions, for example, via measurement of muonium conversion to antimuonium $(\mu^- e^+)$,[1] hyperfine splitting,[2] Lamb shift,[3] or the $1S$-$2S$ atomic transition energy. Muonium is produced by bringing a muon beam to rest in a suitable material, but the subsequent influence of the moderator eliminates many advantages for fundamental investigations of the purely leptonic muonium system. We have observed the decay of muonium atoms in vacuum resulting from emission from a thin layer of finely divided silica powder. This is the most intense source of muonium in vacuum yet reported.

The behavior of muons in silica powder has been studied previously at TRIUMF with use of the spin rotation technique. It has been established that $(61 \pm 3)\%$ of the stopping muons form muonium,[4] a yield similar to that of bulk quartz. The quenching rate of muonium precession by O_2 gas in a silica-powder moderator agrees closely with that in an argon-gas moderator, suggesting that most of the muonium escapes the silica and moves in the regions between the powder grains rather than being trapped inside or at the surface of the grains.[5] In a model where the muonium is formed within the silica grains,

and is expelled into the intergrain region where it diffuses with thermal velocities, a yield of 5% is predicted to be emitted from a thin layer.[6] In addition to silica powder, thermal diffusion and emission into the vacuum of muonium from hot tungsten and platinum foils has been studied.[7] A similar set of experiments performed recently at the National Laboratory for High Energy Physics (KEK) has reported a yield of about 4% from a high-purity hot clean tungsten foil.[8]

Our experimental arrangement is shown in Fig. 1. The M15 low-energy positive-muon channel at TRIUMF[9] delivered 2×10^4 particles/s of nominal central momentum 20.0 ± 0.2 MeV/c and 3% (FWHM) momentum spread through a 13 mm $\times$ 20 mm collimator. The beam was incident at 60° to the normal of a 125-μm plastic scintillator, and transmitted muons then struck a silica-powder-layer target supported on a 2.5-μm Mylar film parallel to the scintillator. The targets studied were two grades of silica powder (3.5- and 7.0-nm particle radius, density 30 mg/cm^3),[10] a powder compressed under 7 tons of pressure to a thickness of 3 mg/cm^2, and an aluminum foil of thickness 3 mg/cm^2 for background estimation. Different thicknesses of uncompressed powder (1 and 3 mg/cm^2) were employed, but fragility of the targets prevented accurate thickness measurements and the layers were not always uniform. The target region was evacuated to a pressure of less than 10^{-6} Torr.
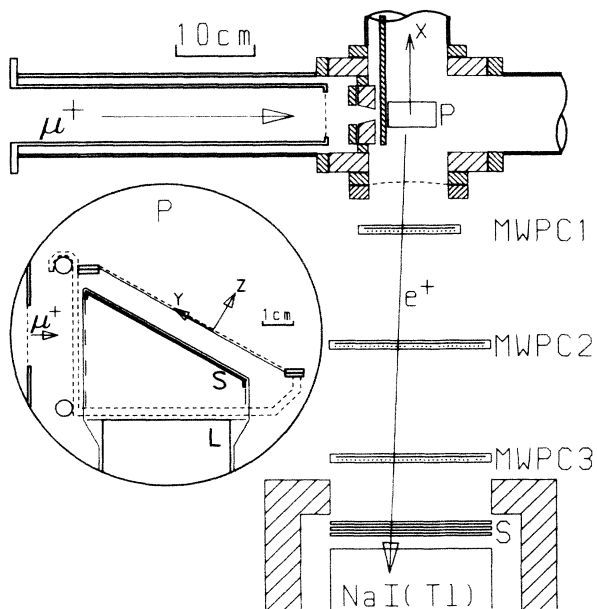
FIG. 1. Schematic of experimental apparatus. The powder target is indicated by P, and S is a stack of three scintillators. Inset: target region as viewed by the wire chambers. The powder layer (P), the thin scintillator (S), and its Lucite light guide (L) are indicated, as are the coordinate axes. Dashed lines indicate structures out of the plane of the beam.

The scintillator-target region was viewed through a 25-μm stainless-steel window by a positron decay telescope consisting of three sets of two-dimensional multiwire proportional chambers (MWPC's), three scintillators, and a large NaI(Tl) crystal. For each event the positron energy, delay time relative to the beam scintillator, and chamber hit coordinates were recorded. The event trigger demanded an incident muon and a positron within a 10-μs interval in MWPC1, the scintillator stack, and the NaI. The NaI clearly recorded the characteristic Michel shape of the muon-decay positron energy spectrum. Events for which one or more muons were incident within 10 μs were rejected to minimize rate-dependent distortion of the muon-decay time spectrum. Figure 2 shows a density plot of the trajectories of the decay positrons extrapolated to the vertical plane containing the beam axis. Decays originating from the target and beam scintillator are clearly seen.

A Monte Carlo simulation has been used to obtain a quantitative understanding of the data. In the simulation model, incident muons are created in the phase space of M15 and undergo collimation, energy loss, and scattering up to their stopping positions. Decays of both in-flight and stopping muons are generated in the direction of the wire chambers. Of those muons stopping in the powder layer, 61% are converted to muonium and undergo a random walk with an effec-
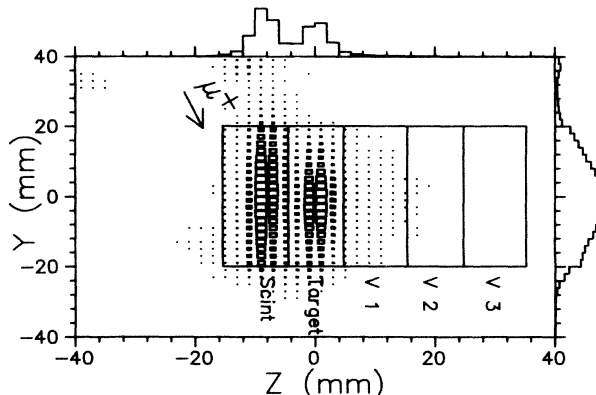
FIG. 2. Density plot of projection of decay-positron trajectory to $x = 0$ plane, showing definition of regions for time histograms. The coordinate axes are defined in Fig. 1.

tive diffusion constant $\mathcal{D}$. The muonium is allowed to escape upon reaching the downstream powder surface with a thermal velocity for 300 K and a cos(θ) angular distribution. Positrons that would undergo large energy losses because of passage through the collimator or window flanges are eliminated. The position resolution of the MWPC track extrapolation is modeled by a Gaussian distribution with a width of 6 mm FWHM determined by the relative intensity of counts in region V1 (region defined in Fig. 2) for the Al foil target and for the simulation with $\mathcal{D} = 0$. The stopping distribution in terms of the ratio of decays in the target to decays in the scintillator is reproduced by adjustment in the simulation of the beam central momentum. The diffusion constant $\mathcal{D}$ is then adjusted to match the ratio of target decays to decays from region V2 of Fig. 2.

Histograms of the observed time of decay for real events in different spatial regions are shown in Fig. 3 for a 1-mg/cm^2 layer of 3.5-nm powder and for the Al foil target, and are compared to the simulation for $\mathcal{D} = 80$ cm^2/s and beam momentum 20.0 MeV/c. Note the nonexponential time dependence introduced by motion of muonium into and out of the different regions. The simulation allows estimates of partial yields for diffusion from the layer followed by decay in each of the four regions, per muon stopping in the silica layer. Based on the measured yield for region V2 of (1.6 ± 0.12)% per stop in the silica, yields into the vacuum of 6.7%, 5.3%, and 0.7% are estimated from the simulation for decays from the target, V1, and V3 regions, with the remainder decaying elsewhere. However, the inferred total yield depends on the input parameters and the model. From simulations with other assumptions, in particular for isotropic emission from the layer, a systematic uncertainty of 30% and a yield of (19 ± 6)% is indicated. The same analysis for a 1-mg/cm^2 layer of 7.0-nm particles gives a similar result while a 3-mg/cm^2 layer of 3.5-nm particles
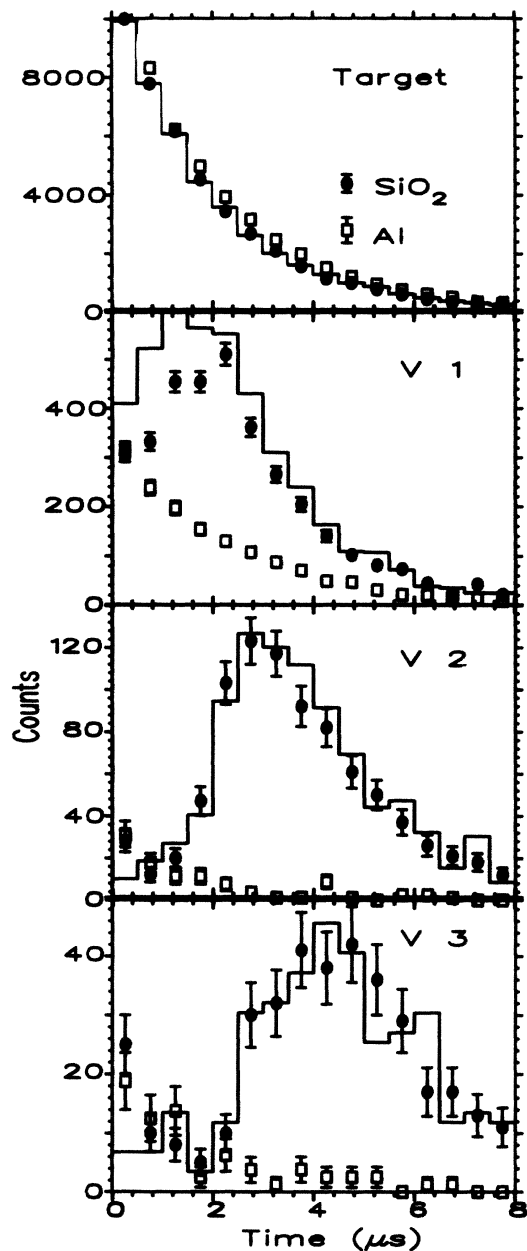
FIG. 3. Muon decay times for events from the spatial regions defined in Fig. 2. Filled circles represent the data from a 1-mg/cm^2 powder, open squares, those from a 3-mg/cm^2 Al foil, and the histograms result from the simulation calculation with diffusion constant of 80 cm^2/s.

yields $(15 \pm 5)\%$.

The background of approximately 40% in region V1 is mainly from muon decay in the target (smeared in apparent position as a result of resolution) which has an almost exponential time dependence. The fit in this region improves for a resolution width of 5 mm rather than 6 mm, without destroying the good agreement in other regions or the calculated yields. Decays in the walls of the apparatus contribute most of the
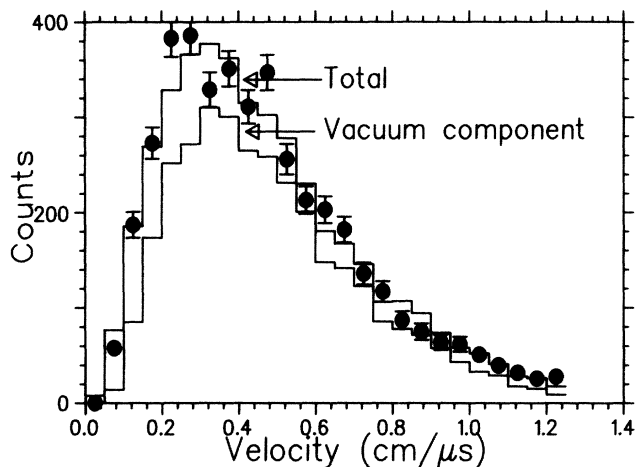
FIG. 4. Velocity distribution of events from spatial regions V1, V2, and V3 for the powder and the simulation as in Fig. 3. Also shown is the component of the simulation from muonium in vacuum.

background in regions V2 (10%) and V3 (25%).

Figure 4 shows a histogram of the distance of the muon from the layer at decay divided by the time of decay (an average velocity during diffusion and drift) for muons decaying in regions V1 and V2. The agreement with the simulation is again very good, confirming the hypothesis of thermal emission. No evidence was noted for a change in yield with an applied electric field of 2.5 V/cm, which is sufficient to inhibit escape of charged muons from the proximity of the layer. This confirms the neutral nature of the signal, while a muoniumlike mass is inferred from the velocity spectrum. Furthermore, the aluminum-foil-target results were well described by the simulation without diffusion where the nonexponential time structures of Fig. 3 are absent. No evidence was noted for muonium emission from the compressed target. We conclude that the effect observed from silica is due to muonium moving at velocities consistent with room-temperature thermal energies.

Some inconsistency was noted with the diffusion model used in the simulation. A thermal diffusion constant $\mathcal{D}$ can be calculated as a function of particle number density and size by treating the layer as a gas of powder particles.[6] For 3.5-nm spheres one obtains $\mathcal{D} = 7.9$ cm^2/s. However, the simulation requires $\mathcal{D} = 80$ cm^2/s, corresponding to a substantially increased yield and indicating the presence of beneficial effects not considered in the model. Our results indicate even higher values of $\mathcal{D}$ for a thicker powder layer. We believe that the primary reason is the existence of large chainlike agglomerates in the powder, regions of higher density separated by large empty volumes, which tend to greatly increase the effective diffusion constant.

Marshall et al.[6] have exploited the advantages of thermal muonium in a search for muonium conversion to antimuonium. Seventeen layers of 3.5-nm-diam SiO_2 powder, each 0.85 mg/cm^2 thick, were used to produce thermal muonium in vacuum. The signal for conversion to antimuonium was a muonic x ray from a CaO surface adjacent to the vacuum drift region. The upper limit obtained on the branching ratio for conversion (with respect to normal muon decay in muonium), 4%, was based on a calculated 5% yield of muonium in vacuum. The present data show that the muonium yield was at least (15 ± 5)% in that experiment. This yield thus places an improved upper limit on this branching ratio of 1% (95% confidence level) and the upper limit on the coupling constant is reduced from 42 to 20 times G_F, the Fermi coupling constant. We are planning an improved muonium conversion experiment at TRIUMF based on radiochemical detection of the μ^-. New measurements of this process have also been proposed at the Clinton P. Anderson Meson Physics Facility (LAMPF), KEK, and the Swiss Institute for Nuclear Research.

(a)Mailing address: TRIUMF, 4004 Wesbrook Mall, Vancouver, B.C. V6T 2A3, Canada.

(b)Mailing address: National Laboratory for High Energy Physics (KEK), Oho-machi, Tsukuba-gun, Ibaraki-ken 305, Japan.

[1]B. Pontecorvo, Zh. Eksp. Teor. Fiz. 33, 549 (1958) [Sov. Phys. JETP 6, (33), 429 (1958)]; G. Feinberg and S. Weinberg, Phys. Rev. Lett. 6, 381 (1961), and Phys. Rev. 123, 1439 (1961).

[2]F. G. Mariam et al., Phys. Rev. Lett. 49, 993 (1982).

[3]C. J. Oram et al., Phys. Rev. Lett. 52, 910 (1984); A. Badertscher et al., Phys. Rev. Lett. 52, 914 (1984).

[4]R. F. Kiefl et al., Hyperfine Interact. 6, 185 (1979).

[5]G. M. Marshall, J. B. Warren, D. M. Garner, G. S. Clark, J. H. Brewer, and D. G. Fleming, Phys. Lett. 65A, 351 (1978).

[6]G. M. Marshall, J. B. Warren, C. J. Oram, and R. F. Kiefl, Phys. Rev. D 25, 1174 (1982); G. M. Marshall, Ph.D. thesis, University of British Columbia, 1981 (unpublished).

[7]K. R. Kendall, Ph.D. thesis, University of Arizona, 1972 (unpublished).

[8]A. P. Mills, Jr., et al., Phys. Rev. Lett. 56, 1463 (1986).

[9]TRIUMF Annual Report of Scientific Activities, 1985 (unpublished). For a history of surface muon development, see T. Bowen, Phys. Today 38, No. 7, 22 (1985).

[10]The powders were kindly furnished by Cabot Corporation, P. O. Box 188, Tuscola, IL, and are described in their technical report. The grades used were EH-5 and M-5.